34. Symposium Solarthermie und Innovative Wärmesysteme
Quarters: Heat Networks / Heat Storage
https://doi.org/10.52825/st-symposium.v1i.1344

Published: 26 Nov. 2024

HYDRA RoS: Large-Scale Production of a Vacuum Tube Collector With an Innovative Hydraulic Design - Robust Manufacturing Process by Rotary Draw Bending and Induction Brazing

Karin Rühling[1], Thomas Weidemann[2], Tony Richter[3], Alexander Wolf[4], Ralf Gritzki[1], Hans-Christian Schmale[3], and Alexander Brosius[4]

[1] TU Dresden, Chair of Building Energy Systems and Heat Supply, Germany

[2] Ritter Energie- und Umwelttechnik GmbH & Co. KG, Germany

[3] TU Dresden, Chair of Joining Technology and Assembly, Germany

[4] TU Dresden, Chair of Forming and Machining processes, Germany

*Correspondence: Karin Rühling, Karin.Ruehling@tu-dresden.de

Abstract. Solar thermal systems, especially in district heating networks, are crucial to achieving climate neutrality in Germany's heat supply by 2045. The joint project HYDRA RoS, funded by the Federal Ministry for Economic Affairs and Climate Protection (Germany), focuses on the development of high-efficiency solar thermal collector concepts for series production with the aim of optimising material and energy use, field hydraulics and control technology. A key component of the project is the use of vacuum tube collectors with CPC (Compound Parabolic Concentrator) reflectors, such as those of RITTER XL Solar. These collectors have proven to deliver high heat yields and can easily reach temperatures of up to 120 °C. The project introduced a new hydraulic register design for these vacuum tube collectors, which improved efficiency and enabled new field interconnection options. However, the new design presented some manufacturing challenges. Finite Element Analysis (FEA) was used to improve the rotary draw bending process and minimise cross-section reductions. Experiments and studies were carried out to achieve a leak-proof connection between the drum connector and the tubes. Computational Fluid Dynamics (CFD) simulations were used to model thermal and fluid dynamic behaviour to guide design optimisation. Prototype collectors were fabricated and tested under controlled conditions to assess their hydraulic and thermal performance. The results show that the new design achieves a significant lower hydraulic loss with the same or a little bit higher thermal efficiencies comparable to the current RITTER XL collector series, while significantly simplifying the manufacturing process.

Keywords: Solar Thermal Collectors, CPC Reflector, Induction Brazing, Rotary Draw Bending, Hydraulic Optimization

1. Introduction and motivation

The transition to renewable energy sources is a critical component in the global effort to mitigate climate change and achieve sustainability. Solar energy, in particular, has emerged as a promising solution due to its abundance, scalability, and environmental benefits. Solar collectors, which convert sunlight into usable thermal or electrical energy, play a pivotal role in harnessing this renewable resource. As the world strives to reduce greenhouse gas emissions

and limit global temperature rise, the steady improvement of solar thermal collector technology has become increasingly important.

However, there are several key challenges in improving the efficiency of the solar collector itselfs and the collector field efficiency. Improving the flow properties and minimising heat transfer pathways is crucial to reducing these thermal losses and enhancing efficiency. Furthermore, the production cost and complexity of some advanced solar collector technologies can be a barrier to their broad acceptance. Balancing performance improvements with cost-effectiveness and simplicity of design is a key challenge in the development of solar collectors. Additionally, ensuring the long-term durability and reliability of solar collectors, especially in harsh environmental conditions, is crucial for their large-scale acceptance. Minimizing the maintenance requirements and improving the robustness of the collectors is an ongoing challenge. Hydra RoS (RoS Register ohne Sammler in German) addresses these challenges by introducing an innovative collector-internal hydraulic design (see Figure 2).

2. Vacuum tube collector CPC-type

2.1. State of the art

CPC-type vacuum tube collectors combine the advantage of the so-called Sydney tube (double-walled, evacuated glass tube with integrated absorber layer) and the enlargement of the aperture area by CPC mirrors with a special design of the heat transfer construction, especially the medium tubes to reach turbulent flow for a very high energy performance.

Previous register concepts typically require so-called "harps" in order to connect a series of tubes/meanders in parallel using one distribution and one collecting tube called manifold each (RmS *Register mit Sammler* in German). This allows larger collector areas to be combined in series in one line in a hydraulically advantageous and cost-effective manner. A disadvantage is the unavoidable asymmetry in the flow induced by the manifold, which can lead to partial stagnation and failure of parts or the entire collector array in the event of unfavourable wiring and conditions (e.g. low flow rate). In addition, many individual cost-intensive production steps and labour-intensive brazing processes are necessary. (see Figure 1)

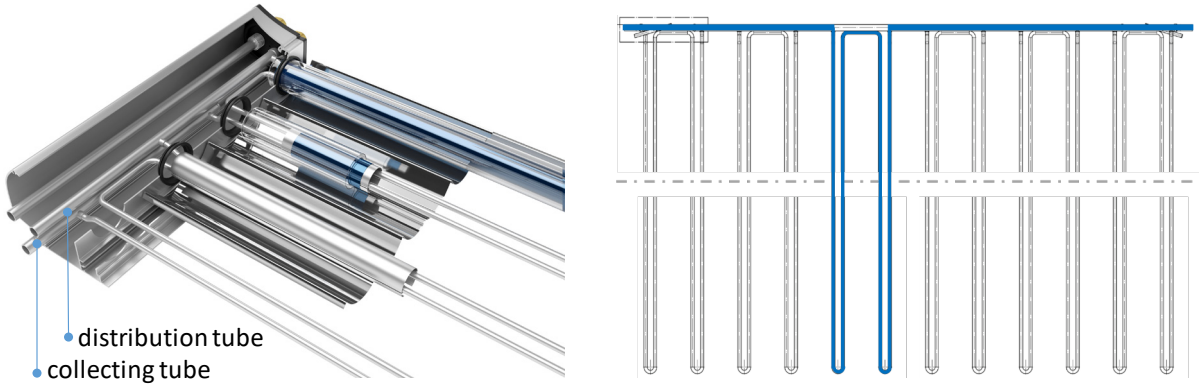

Figure 1. *CPC-type vacuum tube collector – RmS-design*

2.2. New RoS-Design

The central element of the new RoS-Design is the so-called drum connector. The use of drum connectors at the inlet and outlet side of the collector makes it possible completely dispense of distribution or collecting tubes. The special design of several types of meanders allows the connection of up to nine parallel meanders with equal pressure losses. (see Figure 2)

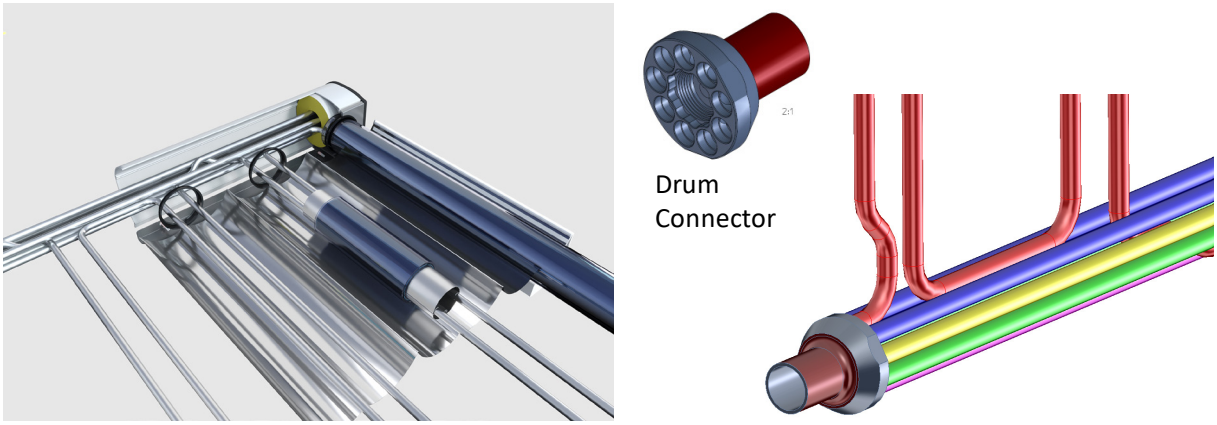

Figure 2. *CPC-type vacuum tube collector – new RoS-design*

The complex bends of the meanders can only be realised in a technically and economically viable way with an automatic tube bending machine. The connection between the tube meander and the drum connector can only be achieved through an automated joining process involving an adhesive bond.

3. Development challenges

3.1. Overview development stages new RoS-design

The way from the detailed construction ideas of the new RoS-collector to a reliable manufacturing process for several 10.000 m² per year required the following development steps:

- Hydraulic optimisation of the inner contour of the meanders and the drum connector using CFD-Simulations
- Development and engineering of a robust rotary draw bending process for small tube diameters and wall thicknesses in different diameters
- Optimisation of the drum connector construction with respect to a long-term stabile brazing joint to the meanders
- Continuous quality assurance of the development process including stress tests in laboratory and field trials and Solar Keymark certification

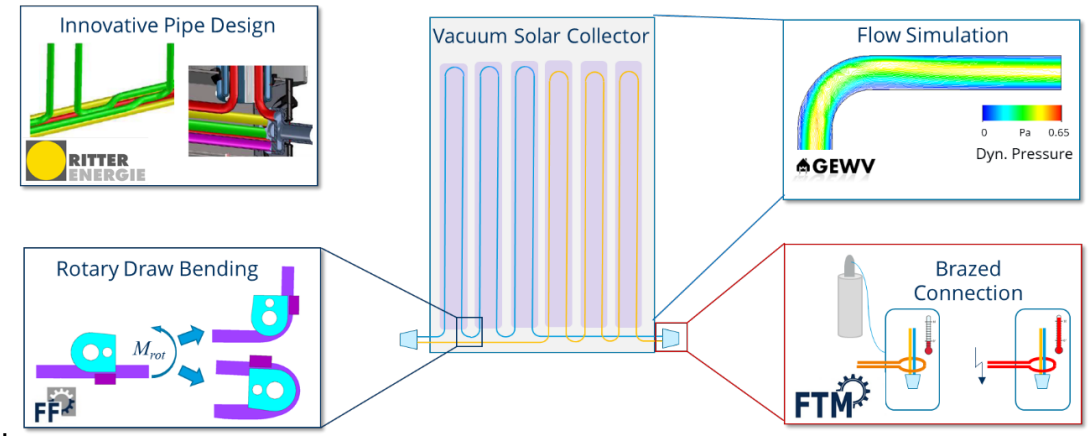

Figure 3. *Establishing steps for the HYDRA RoS development process*

Figure 3 provides a brief overview of the established process and the involved partners. More details regarding the challenges for bending and brazing were discussed in this chapter. An insight in the used investigation methods and results of the development process will be presented in chapter 4.

3.2. Forming challenges

The challenge of improving the heat transfer and length of the tube without enlarging the size of the collector is compounded by the need to manufacture thinner tubes and tighter bending radii. The use of a mandrel is necessary to enable rotary draw bending of tubes with a ratio of the bending radius *r* to the tube diameter *D* below 2, which is just about feasible from a production perspective. A reduction in the tube wall thickness makes the task more difficult, as it is then more likely to form wrinkles and flattened bends which narrow the cross-section to an unacceptably high level, which would result in an increasing pressure loss. When combined with the new proposed bending radius, a point was reached, where robust bending with a constant cross-section was no longer possible. Rotary draw bending can result in the formation of defects such as wrinkling, fracture, and ovality in stainless steel tubes, particularly when the process parameters are incorrectly selected [1]. The degree of ovality, defined as the extent to which a tube deviates from a perfect circle following bending, is influenced by a number of factors [2], including the position of the mandrel, the velocity of the pressure die, the number of balls, and the contact pressure of the pressure die and the friction between the touching surfaces [3]. The discussion of process fluctuations offers a wide range of parameters that may result in the scrap or rework of the parts, for example, due to springback [4]. Recent research has identified some options to compensate for the missing mandrel and allow difficult bends with a near-initial cross-section [5].

3.3. Brazing challenges

The challenge when joining the tubes to the drum connector is to develop a suitable joining process. The following challenges are a consequence of the innovative tube design.

Multiple joints | Simultaneous joining | Automated production

Furthermore, the transfer from the laboratory test rig to the industrial series process must be considered. The connection and the process are subject to requirements such as permanent leak-proofness, dimensional accuracy of the components and high reproducibility. A systematic analysis revealed that the most suitable process for the given circumstances was induction brazing in an inert gas atmosphere. Certain requirements must be met to produce a brazed joint. Firstly, wetting of the base material with solder, afterwards the flow of fillet in the gap must be ensured. The joint is formed because of diffusion and cohesive forces. To fulfil this, a targeted and homogeneous temperature control must be designed. It is essential that the quality characteristics of a brazed joint are achieved and that their verification during production is guaranteed.

4. Methods and important results

4.1. Hydraulic optimization of the inner contour

Simulation studies based on ANSYS Workbench [6] were carried out in preparation for the detailed implementation of the production technology and the commissioning of the new production line. Geometrically high resolved numerical simulations allowed deep insights in the pressure and temperature fields of several construction versions of the whole collector or interesting details by variation the thermal and hydraulic boundary conditions in a widespread way (average velocity inside single meander 0,2 … 1,2 m/s; heat transfer via tube length up to 35 W/m). As expected, the pressure losses in the meander channels dominate the total pressure loss. But hydraulic optimization potential could be identified for the drum connector design for instance, like shown in Figure 4. The minimising of the regions with mean velocities of 1,5 m/s (red coloured) results in significant reduction of the share of drum losses in the total pressure losses from 11,04 % in the basic construction to 5,94 % in the optimized design.

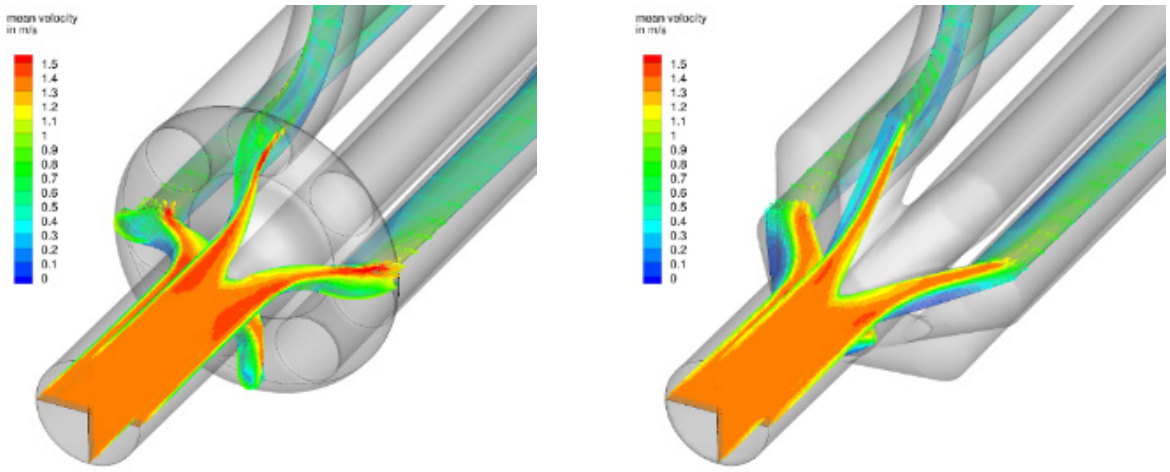

Figure 4. *Results of CFD simulations – Detail of drum connectors and meanders at the inlet side in several sectional plane (velocity meander tube 0,5 m/s, heat transfer 35 W/m tube length); left: basic drum connector construction; right: optimized design*

The simulation based forecast of the overall pressure losses of the whole RoS-collector showed a very good match with the development goals. The comparison with test rig experiment results concerning the pressure loss in dependency of volume flow for several temperatures shows the forecast results in principle. Possibilities of improvement of the simulation models could prove concerning the variation of the values for tube roughness k in dependency of laminar, transitional or turbulent flow like shown in Figure 5.

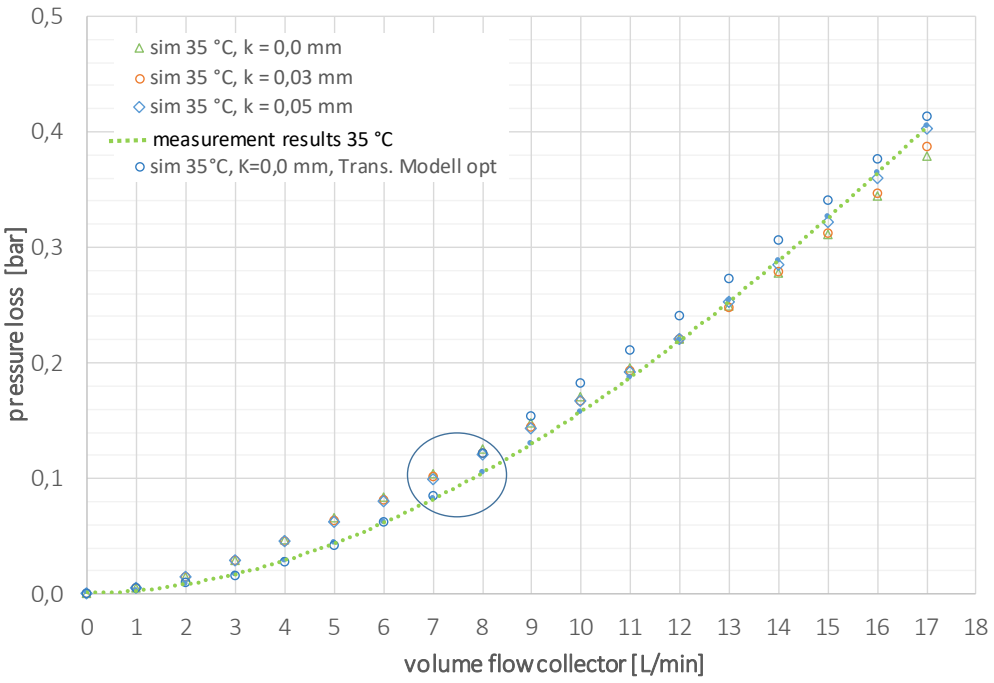

Figure 5. *Pressure loss of new collector 19/49 RoS - comparison of simulation and measurement results for 35 °C water temperature*

4.2. Rotary draw bending of the tube

4.2.1. FEA and experimental setup

By using Finite Element Method (FEM), a deeper understanding of the mechanical behaviour and deformation characteristics that occur during rotary draw bending without a mandrel is gained. This approach enabled the optimization of process parameters with the objective to

minimise defects and achieve the desired bending quality. Furthermore, it allowed the definition of a feasible process window and the resolution of production errors that occurred during the start-up of the new machine. Consequently, it was essential to gain an understanding of the main influencing process factors. Initially, the material parameters were evaluated through tension tests. The tests were conducted on the inspekt250kN tension-compression testing machine from Hegewald&Peschke GmbH with standard clamps. Seven to ten specimens out of different parts of the coil and different batches were performed and a flow curve was generated out of the averaged tests. A Swift approximation was used [7]. The tools were responsibly developed by Schwarze-Robitec GMBH and used the mentioned pre-compression of the tube by a divided bending die to prevent the reduction of the cross section. Furthermore, a clamp die and a pressure die were used and reduced to the main surfaces for the analysis (see Figure 6).

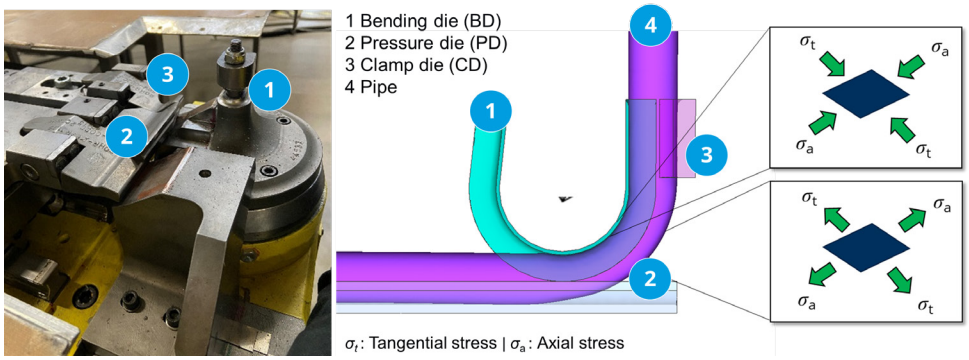

Figure 6. *Setup of the machine and the reduced FE-Calculation with main components*

The calculations were performed with the FE software Simufact.Forming 2016. This was done in three steps. It begins with the closure of the bending, pressure and clamping dies. This is followed by the bending process itself, after which the tools are released. A tube segment with l_{tube} = 150 mm was used. The tube was meshed with hexahedral solid-shell elements with 1 mm initial length, whereas the inner radius of the tube and the area touching the pressure die were meshed with half the initial element length. The pressure die was controlled by path and closed in conjunction with the clamp die in the initial step. The primary process was the rotation of the bending die, which underwent a change regarding the two required bending angles of 90 ° and 180 ° (see Table 1), with the focus of this paper being on the 180 °.

Table 1*. Tested parameter*

Parameter	**Value**	**Parameter**	**Value**
Bending radius *r*	2 * D	Pre-Ovality	115 %
Tube diameter *D*	100 %	Synchro Factor	80 - 100 %
Wall thickness s_0	0.5 mm	Friction μ_{PD}	0.10 | 0.20 | 0.30
Bending angles	90 ° and 180 °	Friction μ_{CD}	0.50
Friction μ_{BD}	0.15	*Gap PD - BD*	0.0 | 0.25 | 0.5 mm

The bending radius *r*, was 2**D* for both bends. The applied pre-ovality was 115 %, whereas the synchro-factor, defined as the velocity quotient of the moved tools, was varied during the analysis. A virtual sensitivity study was conducted to define the usable process window with regard to the cross-section in the centre of the bend and the cross-section of the tube bend itself. This was achieved by testing different friction coefficients and synchro-factor parameter. The results were then compared to those obtained from experiments performed on the newly built machine (see Figure 6). Cross-sections were extracted and embedded in epoxy for comparison with the FEA, with a specific focus on the microstructure and the potential for

bending-induced cracks. Following the validation of the results, a detailed analysis of possible errors in the process was conducted. This was crucial for the prevention of errors in the production. A number of potential errors were identified, including a shift of the dies, an inadequate closing pressure on the dies, and insufficient clearance. In order to assess the robustness of the process, nine different bends were measured for 180 ° and 90 ° (left and right bending direction) using a GOM® Atos Q – System with a measuring volume MV170. The data was processed using ZEISS Inspect suite, 2023.

4.2.2. Results of the FEA and optical measurements

A very good accordance of the result could be reached after a few iterations and refinement of the material model. The calculations showed wrinkling in nearly the same position as in the experimental test whereas the validation of the FE calculation could be stated. Figure 7 shows the comparison of two different bends whereas only the synchro factor was varied by 0.02. This minor deviation in the parameter set results in the formation of wrinkles (Figure 7, red circle) in the tube, marking the upper limit of the process window. After the validation, due to problems with the robustness of the process, the deeper look inside the influencing parameters was performed to establish a stable and reliable process.

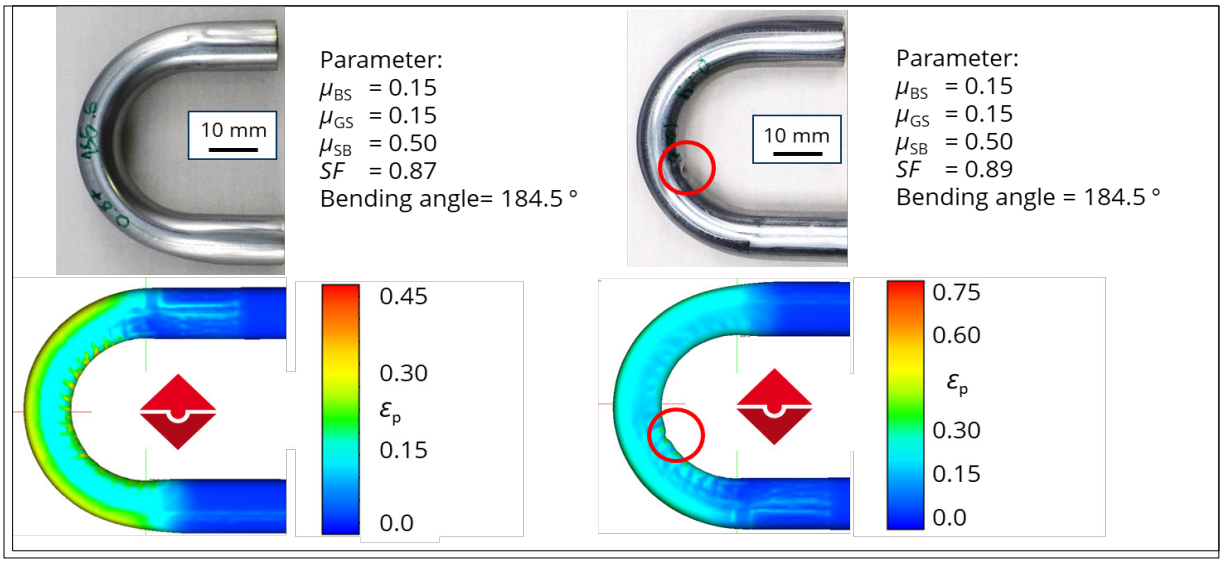

Figure 7. *Validation of the FE calculation by matching experimental results with different synchro factors left and right*

The initial variable to be examined was the feed of the pressure die. Three different feed rates were used (see Table 1). This error may be attributed to an insufficient feeding pressure or mechanical compliance of the tool system. It can be concluded that a full feed is essential for the production of high-quality parts. Conversely, a partial feed may result in the formation of wrinkles on the inner side of the tube due to incomplete pre-ovality. The subsequent parameter under consideration was the friction coefficient of the pressure die. Beginning with μ_{PD} = 0.1 wrinkling could be stated due to insufficient retention force by the pressure die. For μ_{PD} = 0.2 and μ_{PD} = 0.3 wrinkling could be suppressed, although increasing flattening on the outside is detectable.

The resulting sheet thickness t_{tube} of the tube bends showed no critical behaviour. Flattening and wrinkling was a problem but no cracks could be examined in the extracted and embedded section cuts. The minimum thicknesses measured was between 0.409 mm and 0.425 mm for the parameter range from Table 1. This corresponds with the results from the FEA. Furthermore, the analysis has demonstrated that an offset of the tools to each other results in a twisting of the tube meander. As a result, it could be concluded that a good initial alignment is of crucial importance for a stable process.

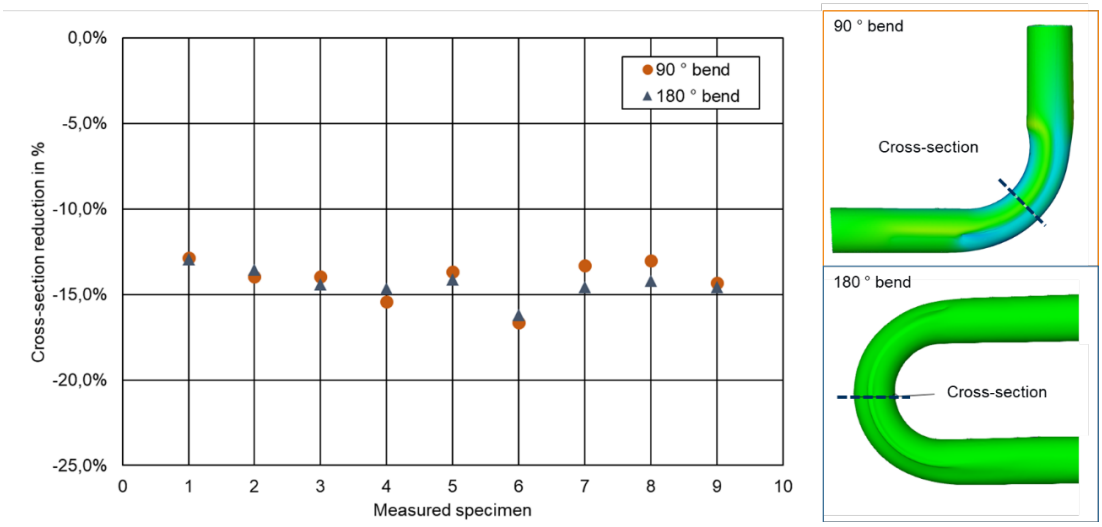

Figure 8. *Measured cross-section deviation in % for the measured specimen (n=9) in the 90 ° and 180 ° bend*

Figure 8 shows the measured cross-section with the resulting values for the different specimen extracted from the produced meander. It is evident that the slight discrepancy from the ideal cross-section is clearly visible, whereas the deviation ranges by approximately -14 %, which is a favourable outcome. The variation is quite small, which was one of the main objectives, whereby the pressure loss is mainly observed in the straight, long sections of the meander. The resulting mean deviation for the 90 ° bend was -14,1 % whereas the 180 ° bends show slightly higher values with a resulting mean deviation of -14,3 %.

4.3. Induction brazing of the drum connector-tube joint

To qualify the brazing process, a laboratory test rig for induction brazing was set up independently, which is shown schematically in Figure 9. The generator is used as the power supply, with the alternating current being passed through a transformer to the water-cooled inductor of one coil. The induced current generated heat for non-contact heating of the drum connector. The energy input depends on the power, frequency and the distance between the inductor and the drum connector. The use of several pyrometers made it possible to qualitatively record the temperature-time curves as well as to ensure that the brazing temperature in the center is reached and the melting temperature in the outer area of the drum connection was not exceeded. A gas chamber was also integrated into the test rig. An inert gas atmosphere was used to prevent oxidation of the base material. To do this, the oxygen content of the atmosphere must fall below a specially determined threshold value. At the same time, the inert gas flow is used to cool the components.

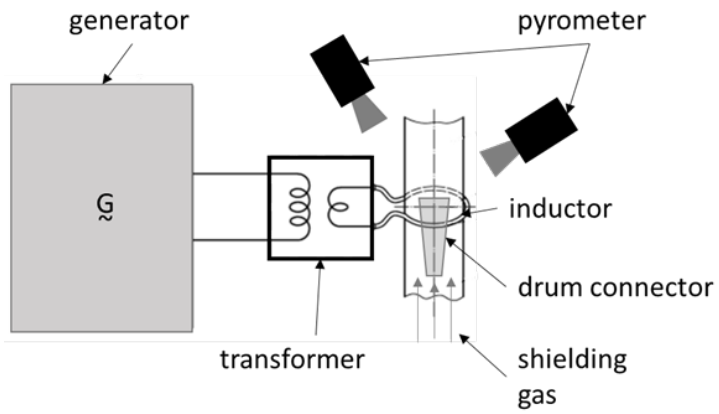

Figure 9. *Schematic laboratory test rig for induction brazing.*

To evaluate the brazed joint cross-sections were made. In order to achieve this, the drum connector was cut in accordance with the specifications outlined in Figure 10a. The metallographic samples were polished using 1 µm diamond papers and subsequently etched using a V2A stain.

The optimized brazing joint from the laboratory test rig is shown in Figure 10. The top view shows the drum connector with seven tubes and in the cross section exposes one of the seven brazed joints. According to DIN EN ISO 18279 [8] the brazed joint shows a small number of irregularities and so the brazed joint is assigned to the strictest quality level. The requirements for leak proofness and dimensional accuracy are fulfilled.

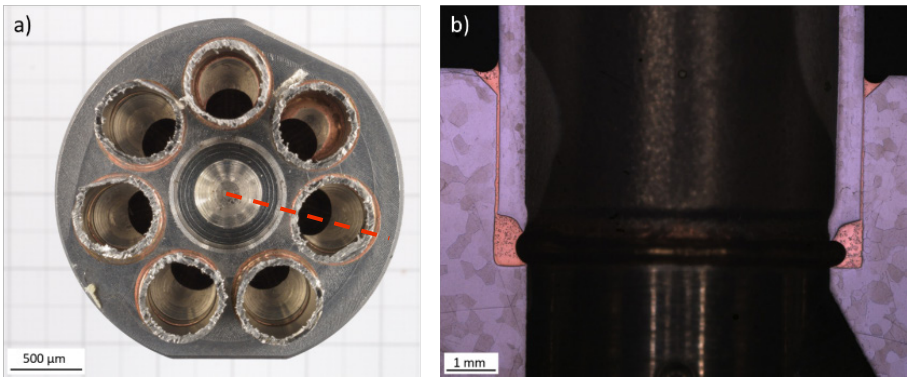

Figure 10. *Result of the optimized induction brazing process. a) top view; b) cross section.*

After the brazing process had been successfully designed, the next step was to check the process stability of the automated induction brazing process. It was checked what happens if the drum connection is positioned slightly incorrectly. Even small changes in the distance between the drum connection and the inductor cause the magnetic field to act differently. As a result, the intensity and depth and the resulting heat input are not homogeneous. On the one hand, the heterogeneous temperature distribution leads to temperature increases, which result in local melting of the base material. On the other hand, the lower penetration depth of the magnetic field causes lower temperatures in the inner area of the drum connector. This results in insufficient wetting of the base material, which leads to bonding and filling defects in the brazing gap. These are shown in Figure 11. The consequence of a temperature change is leaving the process window, that is defined between melting points of the braze metal and the base material. In both cases, the leak proofness of the brazed joint cannot be guaranteed.

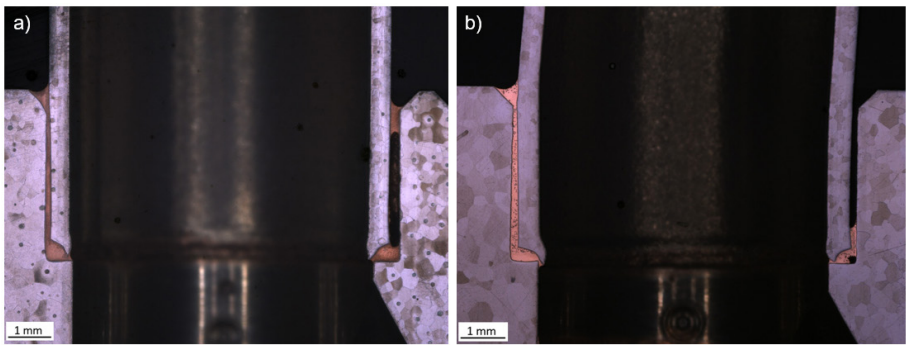

Figure 11. *Irregularities as a consequence of a too low temperature. a) Binding defects; b) Filling defects.*

Geometric deviations of the components and their effects on the automated brazing process were also checked. To simulate machining errors in the tubes or the drum connection, the brazing gap was increased in horizontal direction by skewing the tube and in vertical direction by varying the tube length. If the brazing gap is too big the fillet cannot form the joint and

this results in irregularities and ends in leaks. The cross-sections of these tests are shown in Figure 12. The brazing process compensated a horizontal gap to 1,5 mm (see Figure 12c) and in vertical gap from +1 (see Figure 12a) to -2,5 mm (see Figure 12b). Under these conditions the brazed joint meets the requirement for leak proofness. The reason for this compensation is the control of the heat input, cause the braze metal flows from cold to warm. The brazing process is so designed that the position of the braze metal and the heat input by the inductor is optimized to compensated major geometric changes of the brazing gap.

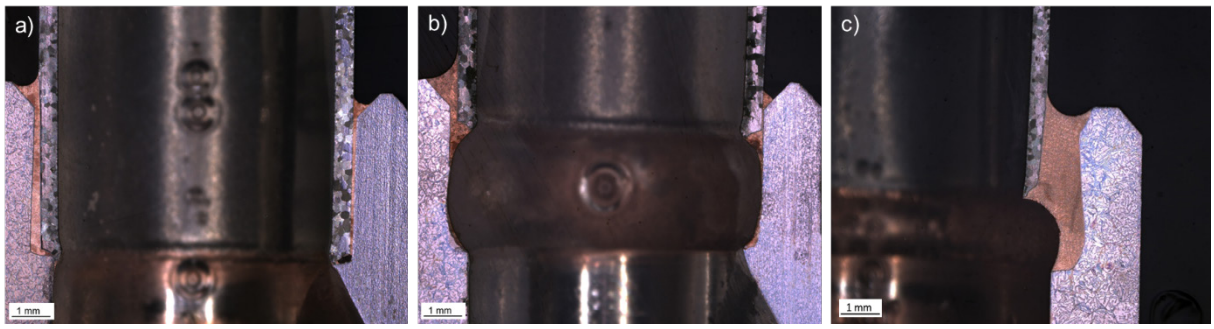

Figure 12. *Cross sections of geometric deviations. a) vertical gap +1 mm; b) vertical gap -2,5 mm; c) horizontal gap +1,5 mm.*

The last step was to define a quality feature for the brazed joint. Requirements for the quality characteristics in an automatic production are a simple and non-destructive method and a regularity whereby leak proofness is matched. A fully formed fillet at the inner site was defined as the quality feature. The fillet also can be easily checked by an optical device and if it is formed the leak proofness is met.

4.4. Field test plant with district heating feed-in

The solar thermal field test plant at the Centre of Energy Technology (CET) of TU Dresden was designed as an indirect solar thermal feed-in substation with water as heat transfer medium at both sides. The feed-in takes place at a decentral place of the primary district heating network of the energy supplier Sachsen Energie AG. The main parameters are given in Figure 13. Primary field test tasks are: proof of correct thermo-hydraulic function of the two parallel collector fields (each nine RoS in series), performance tests for the collector field and daily yield control for the whole plant, followed by intensive resistance tests (artificially induced stagnations with water changes). The innovative control and regulation concept SPSFW [9] of Ritter XL allows stabile feed-in temperatures of 90 °C ± 3 K for the supply line of the district heating network in volatility cases of irradiation, pressure differences at the feed-in point and return line temperatures too.

Main data filed test plant CET

collectortype	Ritter XL 19/49 RoS
numbre of coll.	18
interconnection	2 parallel rows with 9 coll.
gross area	88,92 m²
inclination	25 °
azimut	- 4,81 ° (SSE)
DH Feed-in temp.	$\vartheta_{DH,supply\ line} = 90 \ldots 110$ °C
nominal performance	49,5 kW (1000 W/m² und 60/110 °C DH)
pressure stages	solar thermal side PN10
	district heating side PN25

Figure 13. *Solar thermal field test plant at CET – photo and main data*

Evaluation of the feed-in operation mode for selected hours and the daily yield was carried out following the DIN ISO 24194 [10]. As Figure 14 shows, both tests are successfully passed with an acceptance f_{safe} of 0,9 or better. The realistic f_{safe} for the thermal power output is allocated in the range between 0,9 and 0,95 - depending on the used hour. For the daily yield control, the real values for 2023 are in the range of 0.96.

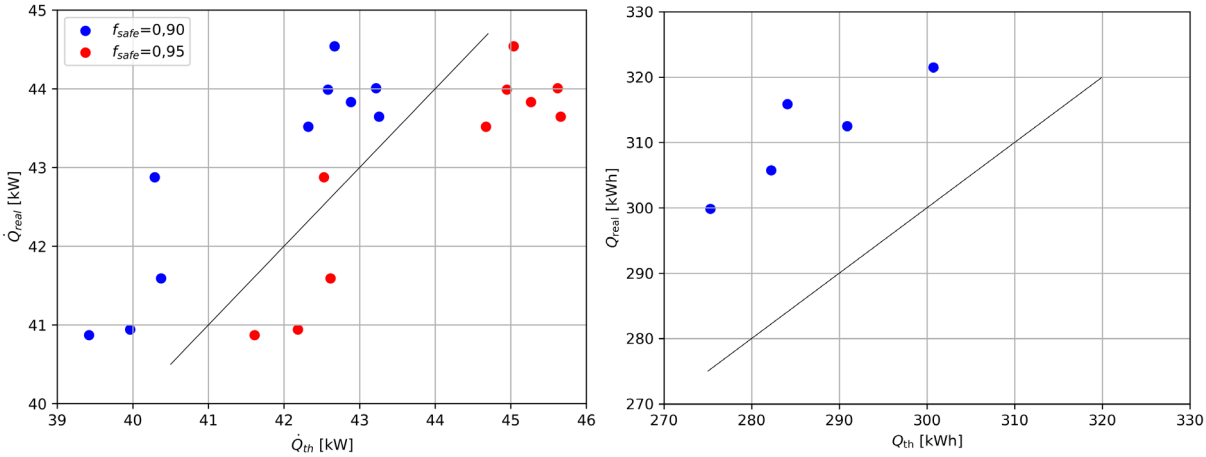

Figure 14. *CET- field test checking results following DIN ISO 24194:2022; left: 10 hours control thermal power output collector field for $f_{safe} = 0{,}9 \wedge 0{,}95$; right: control of daily yield whole plant at the heat exchanger to district heating network for 5 days with $f_{safe} = 0{,}9$ (measured power output $\dot{Q}_{real}$; estimated power output $\dot{Q}_{th}$; daily yield measurement Q_{real}; daily yield estimation of solar thermal system Q_{th}) [11]*

5. Conclusion and outlook

The bending process was analyzed using the FEA, with process limits being set. A validated model was used to calculate possible process deviations and to prepare and apply countermeasures. Following the elimination of upcoming start-up problems and the ramp-up in production, the produced bends were measured optically, with very low deviations in the cross-section of the tube occurring. This verified the robustness and reliability of the process.

An induction brazing process for joining tube registers with a drum connector was successfully designed on a laboratory scale and transferred to an automatic process for series production. This process produces high-quality and reproducible brazed joints. The robustness of the induction brazing process was proven with the help of various error patterns during the transfer to the automatic brazing process. The most important findings are: very precise heat input in the drum connector is extremely important; the brazing process compensates major geometric changes in the brazing gap. A fully formed fillet was defined as a quality feature. All requirements are full filled.

Prototypes of the new RoS vacuum tube collector with CPC were extensively analysed in different laboratory investigation. Nine field test plants of various types (with collector areas up to 90 m²) were successfully completed without any leaks, component failure or glass breakage. The next steps are the start of the series production and the installation of a solar thermal RoS-plant of 2.000 m² with district heating feed-in.

Data availability statement

The data that support the findings will be available in the SOLAR KEYMARK Certificate License No. 011-7S1889 R, No. 011-7S2434 R (https://www.dincertco.tuv.com/?locale=de) and the official final report by the BMWK under the grant numbers 03ETW023A and 03ETW023B following a six-month embargo from the date of publication to allow the commercialisation of research findings.

Author contributions

Karin Rühling: Project administration, Funding acquisition Investigation, Visualization, Validation, Writing Draft; **Thomas Weidemann:** Conceptualization, Funding acquisition, Project administration**,** Resources; **Tony Richter:** Investigation, Visualization, Validation, Writing Draft; **Alexander Wolf:** Investigation, Visualization, Validation, Writing Draft; **Ralf Gritzki:** Formal analysis, Investigation, Visualization, Review & Editing; **Hans-Christian Schmale:** Supervision, Resources, Review & Editing; **Alexander Brosius:** Supervision, Resources, Review & Editing

Competing interests

The authors declare that they have no competing interests.

Funding

The authors would like to thank the Federal Ministry for Economic Affairs and Climate Action (BMWK, Germany) and the Project Management Jülich for the funding and support under grant numbers 03ETW023A and 03ETW023B.

References

[1] A. Mentella and M. Strano, "Rotary draw bending of small diameter copper tubes: predicting the quality of the cross-section," In: Journal of Engineering Manufacture 226, no. 2, pp. 267–278, 2012. DOI: 10.1177/0954405411416306.

[2] H. P. Li, Y. L. Liu, Y. X. Zhu and H. Yang, "Global sensitivity analysis and coupling effects of forming parameters on wall thinning and cross-sectional distortion of rotary draw bending of thin-walled rectangular tube with small bending radius," In: Int. Journal of Adv. Manuf. Techn. 74, pp. 581–589, 2014. DOI: 10.1007/s00170-014-6014-1.

[3] H. Yang, H. Li and M. Zhan, "Friction role in bending behaviors of thin-walled tube in rotary-draw-bending under small bending radii," In: JMPT 210, no. 15, pp. 2273–2284, 2010. DOI: 10.1016/j.jmatprotec.2010.08.021.

[4] H. Li, H. Yang, M. Zhan and Y. L. Kou, "Deformation behaviors of thin-walled tube in rotary draw bending under push assistant loading conditions," In: JMPT 210, no. 1, pp. 143–158, 2010. DOI: 10.1016/j.jmatprotec.2009.07.024.

[5] E. Simonetto, A. Ghiotti and S. Bruschi, "In-process measurement of springback in tube rotary draw bending," In: The International Journal of Advanced Manufacturing Technology 112, 9-10, pp. 2485–2496, 2021. DOI: https://doi.org/10.1007/s00170-020-06453-w.

[6] ANSYS FLUENT INC., "ANSYS FLUENT USER'S GUIDE FOR FLUENT. RELEASE 20.0", 2020.

[7] H. W. Swift, "Plastic Strain in an Isotopic Strain-hardening Material," In: Motor Industry Research Association, 1946.

[8] DEUTSCHES INSTITUT FÜR NORMUNG, "DIN EN ISO 18279" (ISO 18279:2003); Brazing - Imperfections in brazed joints | Hartloeten - Unregelmaessigkeiten in hartgeloeteten Verbindungen, Beuth Verlag GmbH, 2023.

[9] R. Meißner, C. Kettner, S. Bonk, D. Bestenlehner: Modulare Systemsteuerung für solarthermische Heizwerke auf SPS-Basis, 34. Symposium Solarthermie und innovative Wärmesysteme, Bad Staffelstein, 2024.

[10] DEUTSCHES INSTITUT FÜR NORMUNG, "DIN EN ISO 24194/A1, Solar energy - Collector fields - Check of performance | Sonnenenergie - Kollektorfelder - Überprüfung der Leistungsfähigkeit. Änderung 1 (ISO 24194:2022/DAM 1:2023),". EN ISO 24194:2022/prA1:2023, Berlin (Deutsche Norm), Beuth Verlag GmbH, 2023.

[11] T. Sell: Beitrag zur Inbetriebnahme und ersten funktionellen und energetischen Beurteilung der NEST-W 2.0, Dresden, TU Dresden, Professur für Gebäudeenergietechnik und Wärmeversorgung, 2023.